Virus Evolution, 2022, **8(2)**, 1–11
DOI: https://doi.org/10.1093/ve/veac099
Advance access publication date: 14 October 2022
Research Article

Fast-forwarding evolution—Accelerated adaptation in a proofreading-deficient hypermutator herpesvirus

Na Xing,[1] Thomas Höfler,[1,†] Cari J. Hearn,[2,‡] Mariana Nascimento,[1] Georgina Camps Paradell,[1,3] Dino P. McMahon,[3,4] Dusan Kunec,[1] Nikolaus Osterrieder,[1,5] Hans H. Cheng,[2] and Jakob Trimpert[1,*,§]

[1]Institut für Virologie, Freie Universität Berlin, Berlin 14163, Germany, [2]United States Department of Agriculture, Agricultural Research Service, US National Poultry Research Center, Avian Disease and Oncology Laboratory, East Lansing, MI 48823, USA, [3]Institut für Biologie, Freie Universität Berlin, Berlin 14195, Germany, [4]Department for Materials and Environment, BAM Federal Institute for Materials Research and Testing, Unter den Eichen 87, Berlin 12205, Germany and [5]Department of Infectious Disease and Public Health, Jockey Club College of Veterinary Medicine and Life Sciences, City University of Hong Kong, Kowloon, Hong Kong

[†]https://orcid.org/0000-0001-7486-5582
[‡]https://orcid.org/0000-0003-1309-4547
[§]https://orcid.org/0000-0003-1616-0810
*Corresponding author: E-mail: trimpert.jakob@fu-berlin.de

Abstract

Evolution relies on the availability of genetic diversity for fitness-based selection. However, most deoxyribonucleic acid (DNA) viruses employ DNA polymerases (Pol) capable of exonucleolytic proofreading to limit mutation rates during DNA replication. The relative genetic stability produced by high-fidelity genome replication can make studying DNA virus adaptation and evolution an intensive endeavor, especially in slowly replicating viruses. Here, we present a proofreading-impaired Pol mutant (Y547S) of Marek's disease virus that exhibits a hypermutator phenotype while maintaining unimpaired growth *in vitro* and wild-type (WT)-like pathogenicity *in vivo*. At the same time, mutation frequencies observed in Y547S virus populations are 2–5-fold higher compared to the parental WT virus. We find that Y547S adapts faster to growth in originally non-permissive cells, evades pressure conferred by antiviral inhibitors more efficiently, and is more easily attenuated by serial passage in cultured cells compared to WT. Our results suggest that hypermutator viruses can serve as a tool to accelerate evolutionary processes and help identify key genetic changes required for adaptation to novel host cells and resistance to antiviral therapy. Similarly, the rapid attenuation achieved through adaptation of hypermutators to growth in cell culture enables identification of genetic changes underlying attenuation and virulence, knowledge that could practically exploited, e.g. in the rational design of vaccines.

Keywords: polymerase mutant; proofreading deficient; hypermutation; adaptation; DNA polymerase; Marek's Disease Virus.

Introduction

Marek's disease virus (MDV) is a ubiquitous and highly oncogenic alphaherpesvirus of chickens that causes significant economic losses in the poultry industry (Osterrieder et al. 2006). As a member of the *Herpesviridae*, MDV possess a large double-stranded DNA genome (∼175 kb) that encodes for ∼100 gene products (Osterrieder and Vautherot 2004; Gatherer et al. 2021). In contrast to most ribonucleic acid (RNA) viruses, large DNA viruses feature high-fidelity genome replication (Reha-Krantz 2010), mainly achieved through a proofreading function of the viral DNA polymerase (Pol). The DNA Pol of MDV, a protein of approximately 138 kD, is a family B DNA Pol encoded by the viral open reading frame (ORF) U_L30. It contains a 3′-5′ exonuclease (Exo) with conserved domains I–III and is capable of exonucleolytic proofreading (Sui et al. 1995; Trimpert and Osterrieder 2019). Previously, we introduced mutations within these conserved Exo domains of MDV Pol that yielded virus mutants with variable Exo activities that influenced proofreading capability and, thus, mutation frequencies (Trimpert et al. 2019). In this previous study, we generated two mutants within the conserved Exo domain III (Fig. 1), by replacing a conserved amino acid tyrosine with phenylalanine or serine, respectively (Trimpert et al. 2019). The resulting mutants Y567F and Y547S presented highly divergent properties. Exo, and thus proofreading, activity of Y567F was severely impaired, resulting in an eighty-fold higher mutation frequency compared to wild-type (WT) virus in chicken embryo cell (CEC) culture. We found that hypermutator Pol-mutant Y567F generated hyperdiverse populations with quasispecies-like structure within twelve passages following reconstitution, when recovered and grown under permissive conditions. However, the genotype of this virus was highly unstable and showed a strong tendency toward reversion to higher replication fidelity, similar to long-term

Figure 1. Alignment of Exo domain III of selected herpesviruses and other large DNA viruses. The conserved residue Y at position 547 in MDV is marked in red, other conserved residues are displayed in yellow. An asterisk (*) indicates positions that are 100 per cent conserved in the alignment.

passaging in proofreading-deficient coronaviruses (Graepel et al. 2017). By contrast, the Y547S mutant proved to be a slow hypermutator, exhibiting a mutation frequency about three times higher than WT virus in CEC culture. In early passages, it showed WT-like growth kinetics *in vitro* and an *in vivo* disease incidence comparable to WT (Trimpert et al. 2019). These properties make this particular mutant an interesting model for accelerated evolution, as it supplies higher genetic variation for natural selection without turning into a hyperdiverse quasispecies-like population.

In the present study, we employed Pol-mutant Y547S to determine the correlation between mutation frequency and adaptation. To address this question, we adapted both WT and Y547S to replication in permissive CEC culture, as well as to growth in a naturally non-permissive cell line, and determined the phenotype of adapted viruses both *in vitro* and *in vivo* using chickens, the natural host of MDV. Importantly, position Y547 is well conserved among viral family B polymerases, which suggests that similar mutants can be engineered for several other large DNA viruses (Fig. 1). We propose that the use of hypermutators could accelerate evolutionary processes and facilitate the discovery of mutations causing antiviral resistance as well as help elucidate genetic changes underling adaptation to new hosts.

Materials and methods

Ethics statement

All bird experiments were approved by the Avian Disease and Oncology Laboratory Institutional Animal Care and Use Committee (IACUC); approval no. 2019–11 and 2020–01. All chickens were specific pathogen-free (SPF) single-comb, $15I_5 \times 7_1$ white leghorn chickens, a F_1 hybrid cross of Marek's disease (MD) susceptible $15I_5$ males mated to 7_1 females; both lines are highly inbred (Bacon, Hunt, and Cheng 2000).

Cell culture

Primary CECs were prepared from 11-day-old SPF eggs (VALO BioMedia) as previously described (Osterrieder 1999). CECs were maintained in minimal essential medium (MEM; PAN Biotech; Aidenbach, Germany) supplemented with 100 U/ml penicillin, 100 μg/ml streptomycin (AppliChem; Darmstadt, Germany), and 1–10 per cent fetal bovine serum (FBS; PAN Biotech) at 37°C and 5 per cent CO_2. Chicken intestine epithelium T7 cells were cultured in Dulbecco's modified Eagle medium with 10 per cent FBS, 100 units/ml penicillin, and 100 μg/ml streptomycin at 37°C in a 5 per cent CO_2 incubator.

Reconstitution of WT and Y547S mutant viruses

To recover WT virus and the previously generated Pol-mutant Y547S from BAC DNA, a confluent monolayer of CECs in a six-well plate was transfected with BAC DNA extracted with a MIDI prep kit (QIAGEN) from *Escherichia coli* as described previously (Trimpert et al. 2019). Seven days post-transfection, cells from each well were collected and co-seeded with adequate amounts of uninfected CECs onto a 100-mm petri dish. For early passages, 50 per cent of infected cells were used for passaging. When the growth of both viruses became apparent, infected cells were split and 10 per cent of them were used for subsequent passages.

Serial passage of virus on CECs and stock generation

WT and Y547S viruses were subjected to a total of sixty passages (P60) on CECs in 150-mm cell culture dishes. Owing to the strictly cell-associated nature of MDV, virus passage can only be performed by transferring infected cells. To achieve this, infected cells that showed approximately 50 per cent cytopathic effect (CPE) were trypsinized to infect fresh cells with 10 per cent of the previous passage. During long-term passage, CECs were infected by co-seeding uninfected and infected cells or by adding infected cells to a confluent monolayer of uninfected cells. The average passage time in this procedure was 4–5 days per passage. For subsequent experiments or later DNA extraction, virus stocks were generated at least after every 10^{th} passage or when required. To maintain MDV infectivity, infected cells were trypsinized and centrifuged and the cell pellet was re-suspended in 20 per cent FBS MEM; aliquots were transferred to cryotubes and dimethyl sulfoxide was added drop-wise to a final concentration of 10 per cent. The prepared cryotubes were immediately placed in a freezing container filled with isopropanol for at least 24 h at –80°C. Tubes were stored in liquid nitrogen until further use.

Adaptation of viruses to T7 cells

Adaptation of MDV WT and Y547S to T7 (chicken intestinal epithelial cells) (Han, Bertzbach, and Veit 2019) culture was achieved by CEC/T7 co-culture. Initially, CEC/T7 co-cultures were prepared by mixing 25 per cent CECs and 75 per cent T7 cells in a 150-mm petri dish and infected with WT and Y547S from P5 in CEC culture. When 50 per cent CPE was observed, cells were trypsinized and 10 per cent of the infected cells were added to a confluent monolayer of uninfected CEC/T7, in which the number of T7 cells was gradually increased by 10 per cent every five passages. After twelve passages of co-culture, 10 per cent of infected CEC/T7 cells were

used to infect pure T7 cells. Then, the T7-adapted WT and Y547S viruses derived from co-culture underwent an additional twenty serial passages in pure T7 cells, undergoing the same 10 per cent infected cell transfer per passage at approximately 50 per cent CPE described for CEC culture above.

Virus titration

For virus titration, plaque assays were performed on CECs in six-well plates as described previously (Jarosinski et al. 2005). In brief, CECs were infected with serial tenfold dilutions of virus stocks ranging from 10^{-1} to 10^{-6}, followed by incubation at 37°C and 5 per cent CO_2 until plaques were observed (usually 5 days post-infection (dpi)). Next, cells were washed with phosphate-buffered saline (PBS), fixed with 4 per cent formaldehyde, and permeabilized with 0.1 per cent Triton-X 100 for 5 min. Non-specific antigens were blocked by using 3 per cent bovine serum albumin in PBS. Subsequently, cells were stained with anti-MDV chicken serum of dilution 1:2,000 and incubated for 45 min with continuous shaking. After washing with PBS, the second antibody (goat anti-chicken IgG-Alexa Fluor 488) (1:2,000, Invitrogen) was added and incubated at room temperature for 45 min under gentle horizontal agitation. Fluorescent plaques were observed and counted under an inverted fluorescent microscope (Axiovert S100, Zeiss). Titers of each virus were calculated according to plaque counts and dilution.

Multi-step growth kinetics and plaque size assay

Multi-step growth kinetics was performed in duplicates as described previously (Schumacher et al. 2005). To determine virus growth kinetics in CECs, approximately 1×10^6 CECs in each well of a six-well plate were infected with 100 plaque forming units (PFU) of each virus (P10 and P60). Infected cells were trypsinized 1, 2, 3, 4, 5, and 6 dpi and titrated as described above. The same protocol was used for determining growth kinetics of T7-adapted viruses.

To determine cell-to-cell spread of viruses in CECs, plaque size assay was performed as described previously (Jarosinski et al. 2005). Briefly, CECs seeded in a well of six-well plate were infected with 50 PFU of each virus. After 5 dpi, cells were fixed and visualized by staining with anti-MDV chicken serum as described above. Images of fifty randomly selected plaques were taken using an Axio Vert.A1 inverted fluorescent microscope (Zeiss), and plaque areas were measured with ImageJ v.1.53i software (NIH). Then, plaque diameters were calculated and analyzed using Prism 8.0 (GraphPad Software).

Isolation of total DNA from infected cells

For isolation of total DNA from infected cell monolayers (Blin and Stafford 1976), cells were washed with PBS and trypsinized using 0.25 per cent trypsin and 1 mM ethylenediaminetetraacetic acid (EDTA) in PBS. Detached cells were re-suspended in cell culture growth medium and pelleted through centrifugation at $800 \times g$, 4°C for 2 min. Subsequently, the cell pellets were re-suspended with 500 µl of buffer containing 100 mM NaCl, 10 mM Tris, 1 mM EDTA, pH 8.0. After that, 250 µl of sarcosine lysis buffer (75 mM Tris-HCl, 25 mM EDTA, 3 per cent N-lauryl sarcosine, pH 8.0) was added and incubated at 65°C for 15 min. To remove RNA, RNAse A (Promega Corp.) was added and incubated for 30 min at 37°C. Proteinase K (Promega Corp.) was used to digest protein for 16 h at 55°C. Finally, genomic DNA was extracted by phenol–chloroform extraction, precipitated using isopropanol, washed with 70 per cent ethanol, and finally dissolved in diethyl pyrocarbonate (DEPC)-treated water.

Isolation of individual virus genomes

To obtain individual virus whole genome sequences, extrachromosomal DNA was isolated from MDV WT and Y547S-infected CEC cultures at P20 as described previously (Trimpert et al. 2019). Briefly, circular viral genomes were obtained by re-suspending infected cells from one 150-mm cell culture dish in 500 µl PBS followed by lysis using 500 µl Hirt lysis buffer (10 mM Tris-HCl, 20 mM EDTA, 1.2 per cent (w/v) sodium dodecyl sulfate, pH 8.0). The lysate was mixed gently by inverting the tube ten times and incubated for 20 min at room temperature. 250 µl 5 M NaCl solution was added to obtain a final concentration of 1 M NaCl. This salt-rich lysate was incubated at 4°C overnight (>16 h) and centrifuged at 4°C and $15{,}000 \times g$ for 30 min to pellet precipitated protein and chromosomal DNA. The supernatant was removed and used for phenol–chloroform extraction followed by ethanol precipitation of DNA (Sambrook, Russell, and Sambrook 2006). Circular viral DNA obtained by this method was used for the transformation of electrocompetent *E. coli* (MegaX; Invitrogen). Transformed bacteria were plated on lysogeny broth (LB) agar plates containing 15 µg/ml chloramphenicol. Individual clones harboring single-virus genomes were picked after 24–48 h. Clonal viral bacterial artificial chromosome (BAC) DNA was prepared from bacterial clones grown in 5 ml LB overnight using a standard bacterial lysis and phenol–chloroform extraction protocol (Sambrook, Russell, and Sambrook 2006).

Next-generation sequencing and data analysis

Whole genome DNA sequencing was performed on an Illumina MiSeq system. Sequencing libraries were prepared from total cellular DNA extracted from infected cells and produced using the NEBNext Ultra II DNA Library Prep kit (NEB). DNA fragmentation was achieved by using the Covaris M220 focused-ultrasonicator on 1–5 µg of extracted diluted up to 130 µl 0.1 × TE buffer. The size selection step of the NEBNext Ultra II DNA Library Prep protocol was included as to select fragments with a length of 500–700 bp. All other steps were performed as per the manufacturer's instructions. The resulting libraries were enriched for MDV DNA using the myBaits Hybridization Capture for Targeted Next-Generation Sequencing (NGS) kit (Arbor Biosciences) with RNA probes to target the MDV genome as described previously (Trimpert et al. 2017). The hybridization reaction was stopped at the 20 h mark; recovery of the enriched library was performed 'off-bead', and the final polymerase chain reaction cleanup was performed using SPRI Beads (AMPure XP Beads, Beckman Coulter) at a ratio of 0.9 ×. Final enriched libraries were pooled and loaded into the MiSeq instrument as per the Illumina's instructions. Sequencing libraries for individual virus genomes were prepared from BAC DNA isolated from transformed bacterial clones. Clonal BAC DNA did not undergo enrichment for MDV sequences, and libraries prepared using the NEB were sequenced directly. Raw sequencing data and alignments are available at the National Center for Biotechnology Information (NCBI) short read archive, BioProject PRJNA854607.

The generated Illumina sequencing data were processed with Trimmomatic v.0.39 (Bolger, Lohse, and Usadel 2014) and mapped against the MDVvRB-1B reference (accession number: EF523390) using the Burrows-Wheeler aligner v.0.7.17 (Li and Durbin 2009). Mapping statistics were generated using Samtools v1.10 (Danecek et al. 2021), and alignments were visualized using IGV v2.9.4 for Linux (Robinson et al. 2017). For detection of single-nucleotide polymorphisms (SNPs), Freebayes, a Bayesian genetic variant detector, was used. All SNPs with a minimum mapping quality of 5, minimum count of 3, and minimum fraction of 0.01 were considered. Consensus sequences for each sample were

obtained using BCFtools (Danecek et al. 2021). All SNP-containing ORFs sequences were extracted from these consensus genomes and translated using a custom-made script (available at https://github.com/mmnascimento/fastforwardingevolution). This script (Protein_analysis.ipynb) is available as a jupyter notebook and should be opened, edited, and run using jupyter. MDV RB-1B reference files (accession number: EF523390) in FASTA, GFF3, coding sequences (FASTA nucleotide), and protein sequences (FASTA protein) are necessary for this analysis and can be directly downloaded from the NCBI accession page. All parameters for various analytical steps are preset, and only variables for file and reference locations should be edited (under the 'Inputs' section), according to the instructions in the notebook. A version of the notebook complete with recorded variables and outputs from the analysis performed here (MDV_protein_analysis.ipynb) is also available on github.

Plaque reduction assays

To test the sensitivity of WT and Y547S to nucleoside analogue ganciclovir (GCV), a widely used anti-herpesvirus drug, plaque reduction assays were performed in CECs. GCV was purchased as commercial drug preparation (HEXAL AG), and 10 mM stock dilution was prepared by dissolving in sterile water. 100 PFU of WT and Y547S viruses at the early P7 in CECs were used for infection at different concentration of GCV ranging from 40 to 120 μM. Plaque formation was compared to untreated controls. GCV was added whenever medium was changed until the plates were stained for counting plaques. To determine whether sensitivity to GCV decreased after drug treatment, both WT and Y547S at P7 were subjected to ten serial passages in the CEC as described above with the addition of 40 μM GCV in the culture medium. Finally, the drug-treated viruses were used for performing the sensitivity assay as described above. Non-treated control samples were generated from WT and Y547S, which underwent ten serial passages exactly as the treatment groups, however, in the absence of GCV.

Animal experiments

For the *in vivo* animal experiments, SPF chicks without detectable maternal anti-MDV antibody were randomly assigned to different experimental or control groups. To test the correlation between mutation and adaptation, in the first animal experiment, seventeen 1-day-old chicks in each experimental group were challenged with 2,000 PFU of appropriate MDV at different passages (early P10, intermediate P30, and late P60), and the experiment was replicated using the same virus preparations each time. The control group was composed of ten uninfected chicks. Each group was housed separately under standard conditions with appropriate and adjustable temperature and light. Food and water were provided *ad libitum*. The infected animals were monitored on a daily basis over 8 weeks of the experiment, and death or euthanasia of individual chicks was recorded. Chicks were humanely euthanized for significant clinical signs of MD (neuroparalytic disease and/or behavioral depression) according to an IACUC-approved endpoint scoring system. Finally, a thorough postmortem examination was performed on each animal and pathological changes associated with MD including nerve enlargements and tumors in organs were described and recorded.

In the second animal experiment, T7-adapted WT and Y547S at P20 were used for animal infection; again, two independent experiments using the same virus preparation were conducted. All the procedures of the animal experiment were carried out as described above.

Statistical analysis

GraphPad Prism was used for all statistical analysis. Different levels of significance were marked within the figure ($^{*}P \leq 0.05$, $^{**}P \leq 0.01$, $^{***}P \leq 0.001$, $^{****}P \leq 0.0001$). All applied statistical tests can be found in the respective figure legends.

Results

Serial passages of viruses in CECs

Previously, we found that MDV Pol-mutant Y547S (*in vitro* Pol activity: ∼90 per cent of WT, Exo activity: ∼80 per cent of WT) exhibited growth properties similar to WT in the cultured cells and induced MD *in vivo* similar to the parental WT (Trimpert et al. 2019). To further confirm WT-like growth kinetics, two independent biological replicates were examined at P10 in CECs. In both cases, WT and Y547S replicated with very similar kinetics. While Y547S replicated between 1 and 3 dpi with a marginally slower rate, both viruses reached similar peak titers at 4 dpi (Fig. 2A). To determine whether mutation load increases with *in vitro* passaging and how this relates to attenuation of this initially highly pathogenic virus, we serially passaged WT and Y547S sixty times in CECs, performing two independent biological replicates for each virus. At P60, WT and Y547S of both replicates exhibited very similar growth in CECs, with no significant differences observed at any time point (Fig. 2B) and caused comparable CPE (Fig. 2C). NGS data demonstrated that approximately twice as many mutations (cutoff at 10 per cent of sequence reads) accumulated in Y547S compared to WT virus populations by P60 (Fig. 3A, Supplementary Table S1). To ascertain significantly higher mutations rates in Y547S, justifying its designation as hypermutator compared to WT, we next assessed the accumulation of mutations in individual virus genomes at P20 in CEC culture (Fig. 3B). Owing to the metastable nature of the bacterial origin of replication contained in our BAC-derived MDV, P20 was the last passage in which clonal genomes were easily obtained. At the individual level, we found mutations to accumulate significantly faster in Y547S compared to WT (Fig. 3C) and at an average rate of 0.67 per passage, which is approximately ten times faster compared to the WT (Supplementary Table S2). Compared to the growth kinetics measured for P10, we observed adaptation in both viruses trending toward faster and prolonged growth in CECs (Fig. 2B). A non-significant trend toward higher titers was observed in both WT replicates at P60. However, Y547S maintained WT-like growth, while at the same time its mutation load remained stably elevated compared to WT (Figs 2 and 3A).

Adaptation to a non-permissive chicken epithelial cell line (T7)

Few cell lines support the growth of MDV *in vitro* (Witter 2001). Therefore, MDV is typically grown on primary cells such as CECs, duck embryo cells, or chick kidney cells (Biggs 2001). To test the adaptability of WT MDV and Y547S to naturally non-permissive cells, we made use of a chicken intestinal epithelium cell line-designated T7 (Han, Bertzbach, and Veit 2019) that normally does not support MDV replication (Supplementary Fig. S1). To determine whether WT and Y547S viruses can adapt to growth in T7 cells, to assess mutation frequencies under the selective pressure of adaptation to a novel environment, and to test whether adaptability is a function of mutation frequency, we attempted to adapt both viruses to T7 cells. Indeed, both WT and Y547S could be adapted to T7 cells and started to produce visible CPE on pure T7 cell cultures after just twelve passages of growing in CEC/T7 co-culture (Fig. 4A). However, growth on T7 cells (Fig. 4B) was slower

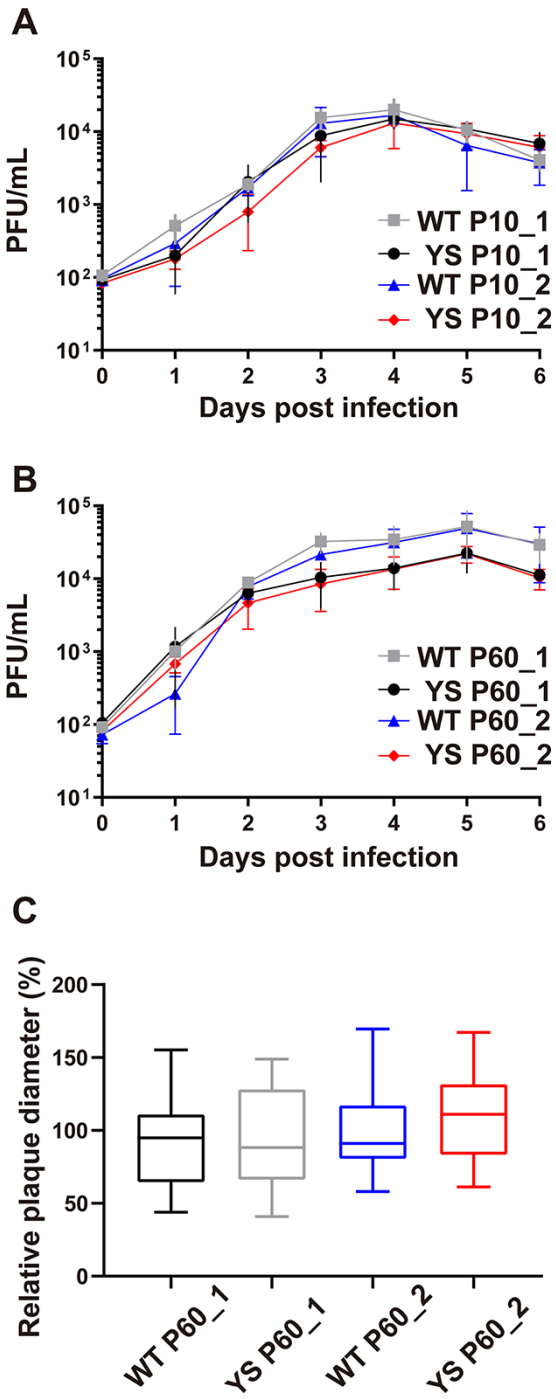

Figure 2. Multi-step growth kinetics of WT and Y547S mutant virus reveal adaptation to CEC culture. Confluent CEC monolayers were infected with 100 PFU of WT or Y547S virus from different passages and replicates. Virus progeny at the indicated dpi (day 1–6) was collected and used for titration. (A) Growth curves of WT and Y547S virus at early P10 of two replicates as well as (B) growth curves of WT and Y547S virus at late P60 of two replicates are shown. Titers are shown as mean ± standard deviations (SD) of three independent experiments. There were no statistical differences between WT and Y547S calculated by two-way analysis of variance (ANOVA) followed by Bonferroni post-test. (C) Plaque size measurement of WT and Y547S mutant virus at P60 from two independent replicates. The box plot shows the relative plaque diameter normalized against the average plaque diameters of WT ($n = 50$; $P > 0.05$, Unpaired t test).

compared to growth on CECs (Fig. 2A, B). After twenty passages, Y547S replicated faster and to significantly higher titers than WT at late time points post-infection (Fig. 4C). In turn, both viruses, adapted to growth on T7 cells following twenty passages on these cells (P20), grew to approximately ten-fold lower titers on CEC compared to the parental virus prior to T7 cell adaptation, without appreciable differences between both viruses (Fig. 4D). This indicates a trade-off between replication on T7 cells and CECs. NGS revealed that Y547S accumulated about five times more mutations than WT (Fig. 5, Supplementary Table S4), which suggests that the hypermutator may adapt faster to a new environment, possibly by accumulating more beneficial mutations. Selection of beneficial mutations is suggested by the much higher abundance of novel majority variants that occur in >50 per cent of the sequenced population (5 for WT vs. 30 for Y547S at P20 on T7 cells, Supplementary Table S4). Interestingly, penetrant and thus potentially strongly adaptive changes (occurring in >90 per cent of the viral population) are concentrated in MDV072 (LORF11) for the WT. At the same time, this is the only ORF in which high-level mutations independently occur in both the WT and Y547S, suggesting an important role of this unique and not well-characterized gene for host cell tropism of MDV (Lee et al. 2007). Other potentially strongly adaptive changes with high penetrance were more frequently observed in Y547S (Supplementary Table S4), suggesting hypermutating viruses can be utilized for identification of genetic changes that underlie various viral adaptations. Additionally, sequencing confirms that the observed mutation frequency in a novel environment is higher compared to the mutation frequency observed in a conserved environment such as CEC culture. While this is true for both WT and Y547S, the hypermutator phenotype of Y547S, in comparison to WT, is more pronounced in the novel environment (Supplementary Table S6). Generally, we observe a trend toward decreased accumulation rates (mutations/passage) of mutations at later passages (Supplementary Table S6).

Adaptation to antiviral treatment

To test the adaptability of our viruses to a different selective pressure, we passaged parental WT and Y547S viruses ten times in the presence or absence of sub-inhibitory concentrations of the nucleoside analogue GCV (GCV, 40 μM), to determine whether viruses would be selected for increased resistance and if Y547S gained resistance to GCV more easily than WT. GCV-treated or non-treated WT and Y547S at P10 were subject to plaque reduction assays to measure antiviral resistance. Both WT and Y547S showed increased resistance to GCV after ten passages of drug treatment compared to untreated controls (Fig. 6). Again, Y547S displayed higher resistance to GCV than WT at P10, which indicates more efficient evolution of resistance to antiviral treatment. This coincides with higher mutation frequencies observed for Y547S (Fig. 7). Importantly, coding mutations were more frequently observed in genes known to be involved in the development of drug resistance, such as U_L30, which encodes the DNA Pol (Supplementary Table S5).

In vitro adaptation and mutation load correlate with attenuation *in vivo*

Adaptation to CEC leads to more proficient replication *in vitro* for both WT and Y547S, with the former performing even slightly better than the latter. It is known that serial passaging of MDV in CEC culture causes attenuation *in vivo* (Hildebrandt et al. 2014). We could recently show that *in vitro* diversification of a hypermutator (Pol Y567F) MDV population led to an increase in virulence (Trimpert et al. 2019). However, and contrary to the situation observed for Y547S, Pol-mutant Y567F has little proofreading activity left and exhibits a suicidal phenotype in CEC

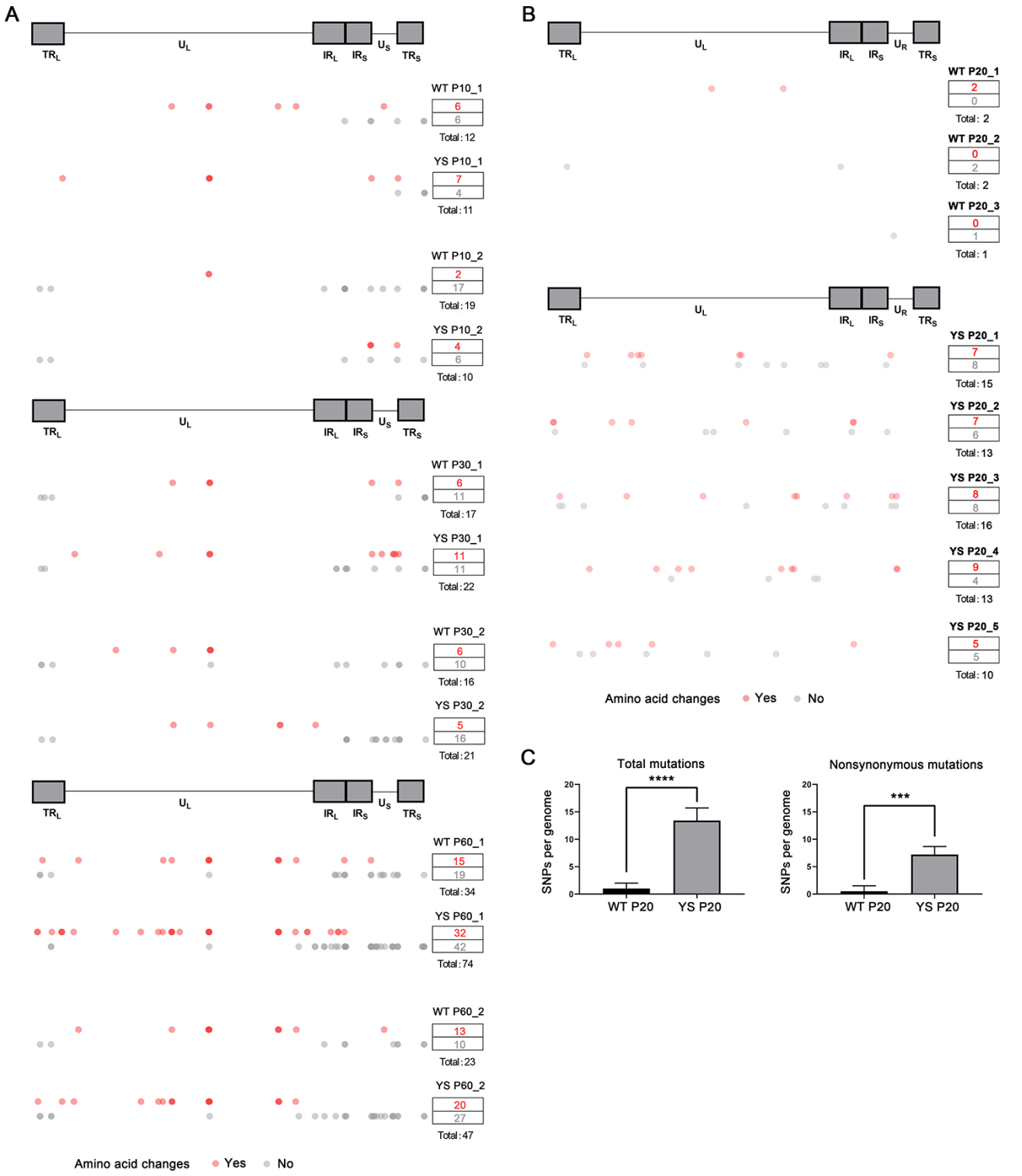

Figure 3. SNPs in independently generated virus populations or clonal virus genomes derived from CEC-adapted viruses. (A) Distribution of mutations in populations of CEC-adapted viruses at P10, P30, and P60 and (B) Distribution of mutations in clonal viral genome isolated from P20 in CEC cell culture, show steadily elevated mutation load in the Y547S hypermutator. The MDV genome consists of a unique long segment (U_L) and a unique short segment (U_S) flanked by a long terminal repeat and a long internal repeat (TR_L and IR_L, respectively) and by a short terminal repeat and a short internal repeat (TR_S and IR_S, respectively). Mutations are displayed as red dots if non-synonymous (i.e. results in an amino acid change) or grey if synonymous or non-coding. The total number of mutations for each virus, passage and replicate are summarized on the right side of the figure. (C) Total mutations and non-synonymous mutations in clonal viral genomes isolated from WT ($N = 4$) and Y547S ($N = 5$) at P20 in CEC cell culture. Asterisks indicate significant differences between WT and Y547S (*** $P \leq 0.001$, **** $P \leq 0.0001$, Mann–Whitney U test).

culture, unless maintained at large population sizes, which allow formation of hyperdiverse populations with stable replication (Trimpert et al. 2019). To determine the effect of comparatively slow but steady hypermutation in a virus that shows an otherwise WT-like phenotype, we aimed at determining virulence *in vivo* following CEC passages. To this end, we infected 1-day-old chicks

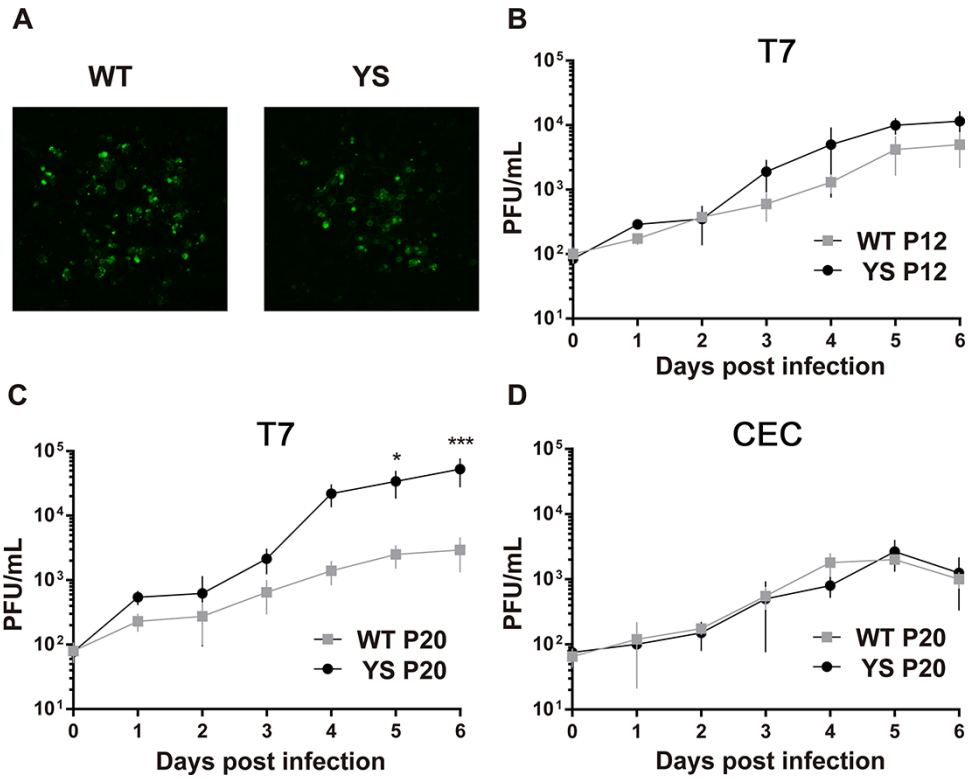

Figure 4. Faster adaptation of Y547S to T7 cells compared to WT. (A) Representative plaques of T7-adapted viruses on T7 cells (B, C) Multi-step growth kinetics of WT and Y547S virus from P12 (B) and P20 (C) in T7 cells. (D) Comparison of multi-step growth kinetics of T7-adapted viruses WT and Y547S at P20 in CEC. The asterisks indicate statistically significant differences (*$P < 0.05$, **$P < 0.01$, ***$P < 0.001$, ****$P < 0.0001$) between WT and Y547S calculated by two-way ANOVA followed by Bonferroni post-test.

with 2,000 PFU of WT and Y547S virus from P10, P30, as well as P60 and monitored them for signs of MD in the following 8 weeks. Here, based on a scoring system with defined humane endpoints (MD stage 4), chickens that showed significant neurological impairment and/or behavioral depression rendering them unlikely to eat and drink adequately were humanely euthanized. Occasionally, birds died acutely without reaching humane endpoint criteria. However, since MDV infection may cause relatively late tumorigenesis with affected animals surviving longer than 8 weeks, we included tumor incidence determined at final necropsy as a secondary readout in our analyses. Survival curves of birds in two independently trials showed successive loss of virulence with increased CEC passages for both, WT and Y547S (Fig. 8A–D). Apart from a reduction of lethal outcomes, we also observed a decrease in tumor incidence, more so in Y547S than in WT. Indeed, Y547S at P60 was fully attenuated and did not cause any disease in one of the replicates (Fig. 8E, F). These results strongly suggest an attenuation of *in vitro* passaged viruses, specifically for Y547S, which also accumulated considerably more mutations upon *in vitro* passaging. To further demonstrate the attenuating effect of adaptation to a novel environment, in our case adaptation to an initially non-permissive cell line, we next used T7 cell-adapted viruses in the same experimental setup *in vivo*. In this scenario, only twenty passages on T7 cells lead to an outcome similar to sixty passages on CECs (compare Figs 8–9). Importantly, Y547S passaged on T7 cells became completely avirulent within only twenty passages with none of the subjects showing any sign of MD (Fig. 9C, D). Taken together, our *in vivo* results confirm not only that *in vitro* adaptation leads to attenuation; more than that, they demonstrate that hypermutation by means of impaired DNA proofreading, especially when combined with adaptation to a novel environment, drastically accelerates attenuation upon *in vitro* passaging.

Discussion

Genetic variability is a prerequisite for natural selection and thus the basis of evolution. Mutation is the mechanism through which genetic variability is generated, while the phenotypic diversity encoded by genetic variation facilitates selection, enables adaptation, and empowers organisms to survive and possibly excel in changing environments. However, given the random occurrence of mutations, the likelihood of interference with important functions is substantial, meaning that high mutation rates are not necessarily beneficial, especially in conserved environments (Loewe and Hill 2010). Regulating the mutation rate therefore becomes essential to allow adaptability while ensuring functionality. Here, we report the behavior of a stably replicating hypermutator (Y547S) with about 2–5 times higher mutation frequency compared to WT on a population level. Results obtained from sequencing of individual virus genomes indicate an even higher mutation frequency in individual Y547S genomes, thus justifying its classification as hypermutator. Throughout our experiments, we found that Y547S retained stable growth and increased mutation rates without showing a tendency toward reversion. These properties distinguish this mutant from other Exo mutants generated by us and make MDV Pol-mutant Y547S an ideal tool to study the longer-term consequences of moderately accelerated mutation rates. In

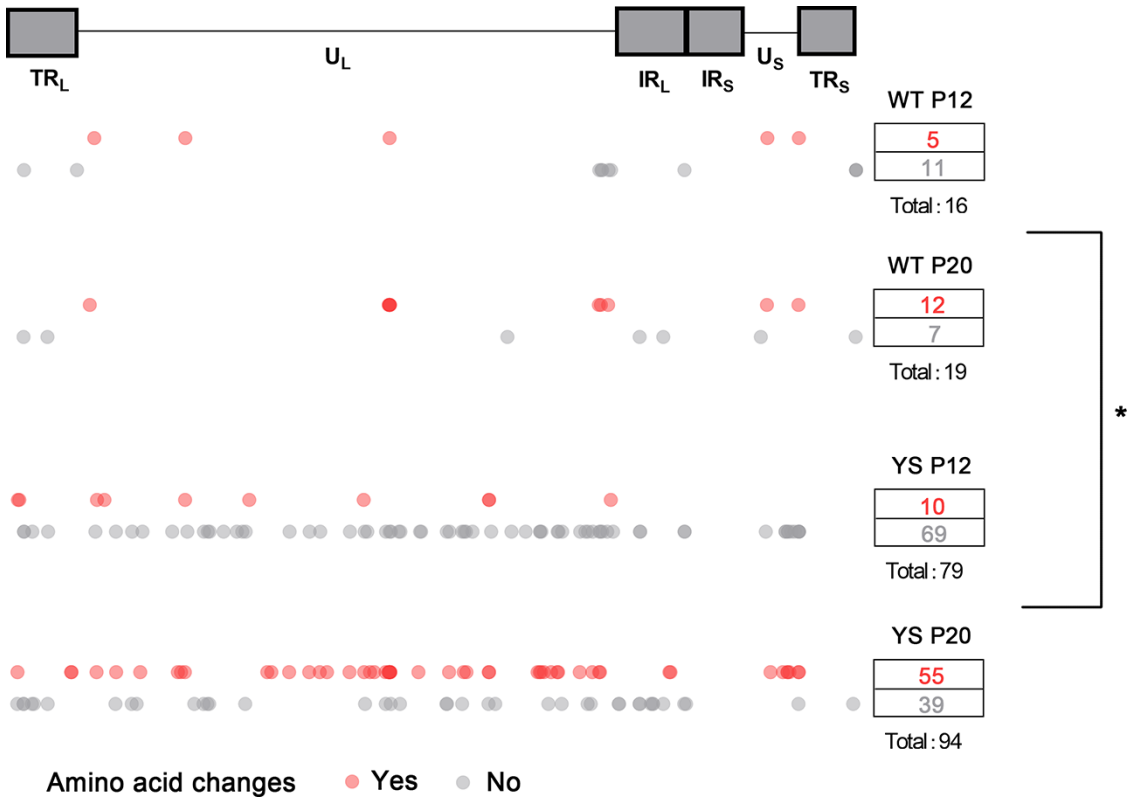

Figure 5. Distribution of mutations in the genomes of T7-adapted viruses from P12 and P20 show over baseline elevated mutation load in Y547S hypermutator. A schematic representation of the MDV genome showing the distribution of the mutations identified in T7-adapted WT and Y547S. U_L: unique long segment; U_R: unique short segment; TR_L: long terminal repeat; IR_L: long internal repeat; TR_S: short terminal repeat; IR_S: short internal repeat. Mutations are displayed as red dots if non-synonymous (i.e. results in an amino acid change) or grey if synonymous. The asterisk indicates significant differences in total mutation rates between WT and Y547S (* $P < 0.05$, Unpaired *t*-test).

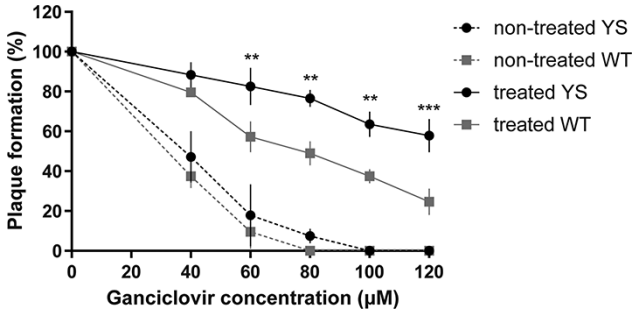

Figure 6. Sub-inhibitory GCV treatment leads to increased resistance, especially in the Y547S hypermutator. Plaque reduction assay of WT and Y547S from P10 without or with GCV selection performed on CECs. Data are shown as the mean of three independent experiments with SD. The asterisks indicate statistically significant differences (** $P < 0.01$, *** $P < 0.001$) between WT and Y547S. Two-way ANOVA followed by Bonferroni post-test was applied for statistical analysis.

several experimental setups, we found the hypermutator to be capable of overall faster adaptation, specifically when exposed to novel environments.

Passaging of initially similarly replicating WT and Y547S viruses on CECs resulted in adaptation to *in vitro* growth conditions with the WT trending toward higher replication rates compared to the Y547S hypermutator. Considering that the virus used in our study is derived from an isolate propagated in the CEC culture (Petherbridge et al. 2004), we consider these cells to be a conserved environment in which these viruses are well adapted. Overall similar growth with a trend toward better performance of the WT upon long-term culture is unsurprising in this benign environment. The higher mutation rate of Y547S leads to more mutations which accumulate over time in the population without providing significant growth advantages. Relative genetic stability, exemplified by thirty-four mutations in WT compared to seventy-five mutations in Y547S after sixty passages, appears to be not detrimental in such an environment.

However, upon introduction of selective pressure such as antiviral treatment with nucleoside analogues, faster adaptation, in this case development of drug resistance, can be observed for the hypermutator and is also reflected by a greater number of mutations positively selected in relatively short time. Similarly, hypermutation is also linked to faster development of drug resistance in bacteria (Blazquez 2003; Macia et al. 2005; Sheng et al. 2020).

The advantage conferred by higher mutation rates becomes even more apparent if viruses are adapted to growth in a somewhat novel and less permissive environment. T7 cells, isolated from the intestinal epithelium of chickens (Han, Bertzbach, and Veit 2019), are naturally non-permissive to productive infection with MDV. Cultivation of virus on CEC/T7 co-culture allows MDV to jump to the new cell line and adapt to replication in a formerly non-permissive environment. In such a scenario, the hypermutator may be able to adapt faster and more efficiently to the conditions and challenges presented by a foreign host cell when compared to WT. Here, the ninety-four mutations observed for Y547S appear to convey a greater fitness advantage compared to only nineteen mutations observed for WT. Interestingly,

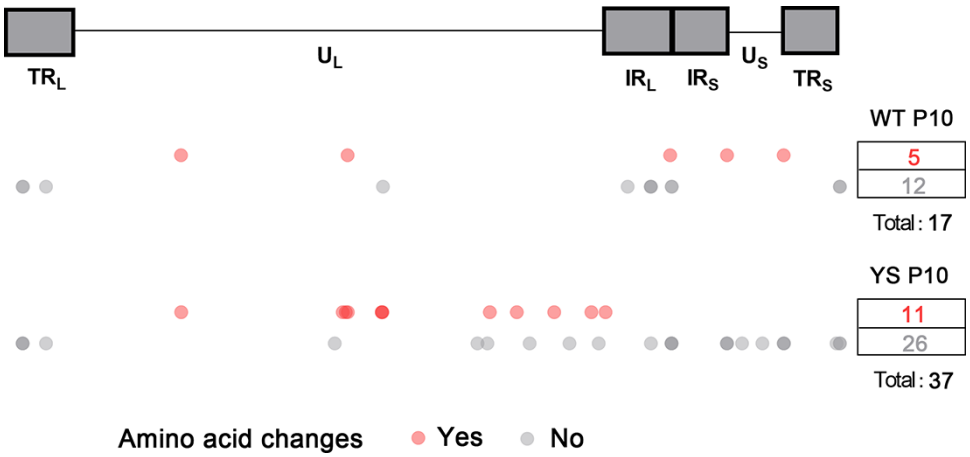

Figure 7. Distribution of mutation in genomes of viruses that were propagated in CECs ten times in the presence of GCV. Mutations are displayed as red dots if non-synonymous (i.e. results in an amino acid change) or grey if synonymous.

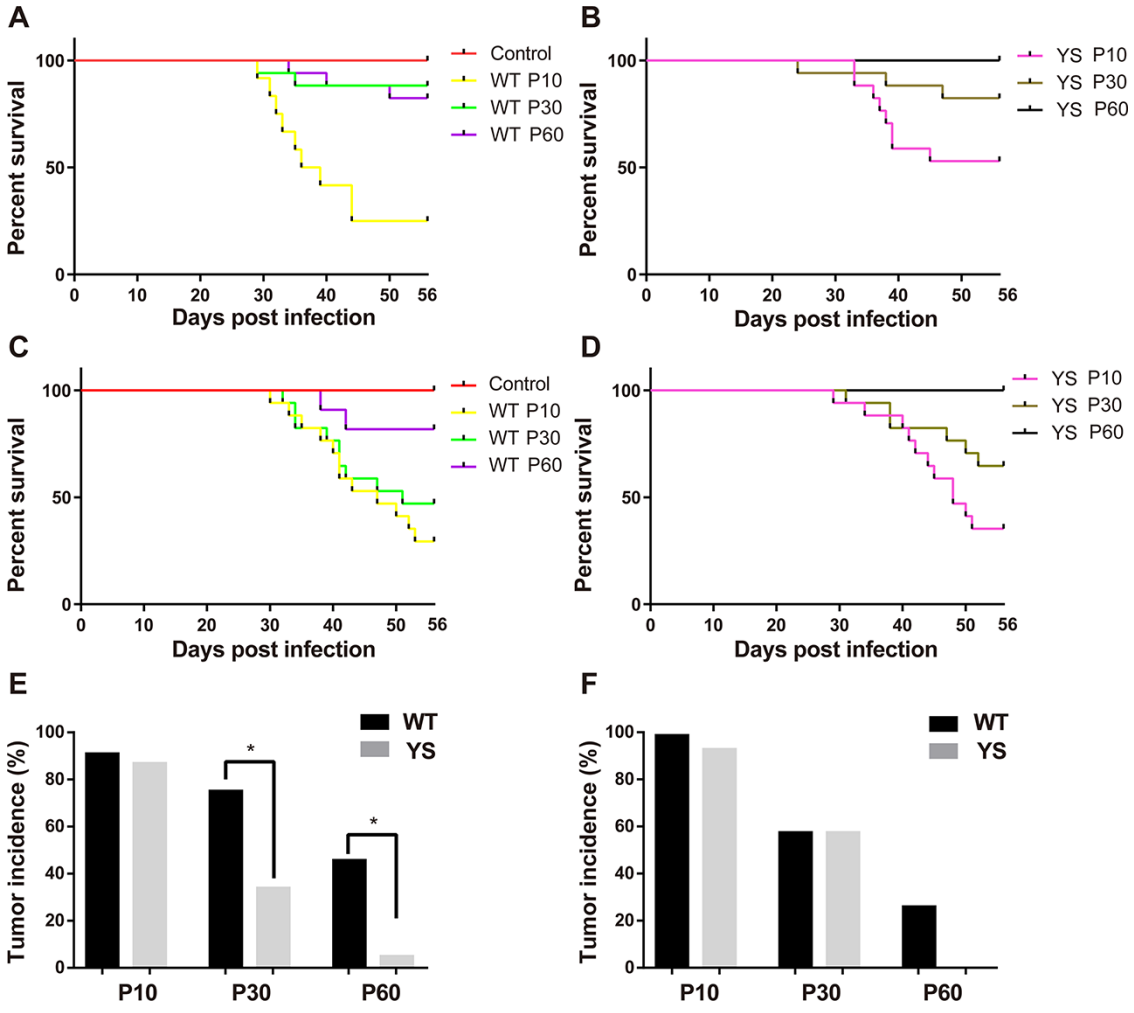

Figure 8. Survival curves and tumor incidence of chickens infected with different passages of CEC-adapted WT and Y547S viruses. Chickens were infected with the indicated viruses and monitored for up to 8 weeks. Spontaneous death or humane endpoint euthanasia due to MD were recorded. Survival curves for the first replicate of WT and uninfected controls (A) and Y547S (B) viruses are shown. Chickens were infected with indicated viruses at P10, P30, and P60 of the first replica of CEC-adapted viruses. Animal numbers: WT P10 = 13; WT P30 = 17; WT P60 = 17; YS P10 = 17; YS P30 = 17; YS P60 = 16, control (uninfected) = 10. Survival curves for the second replicate of WT (C) and Y547S (D) infections are shown. Chickens were the same virus preparations. Animal numbers: WT P10 = 17; WT P30 = 17; WT P60 = 11; YS P10 = 17; YS P30 = 17; YS P60= 17, control (uninfected) = 10. Tumor incidences from the first (E) and second (F) replicate are shown as the percentage of affected chickens in each group. Asterisks indicate significant differences (* $P < 0.05$, Fisher's exact test). Please refer to Supplementary Table S7 for a detailed overview of the animal experiments.

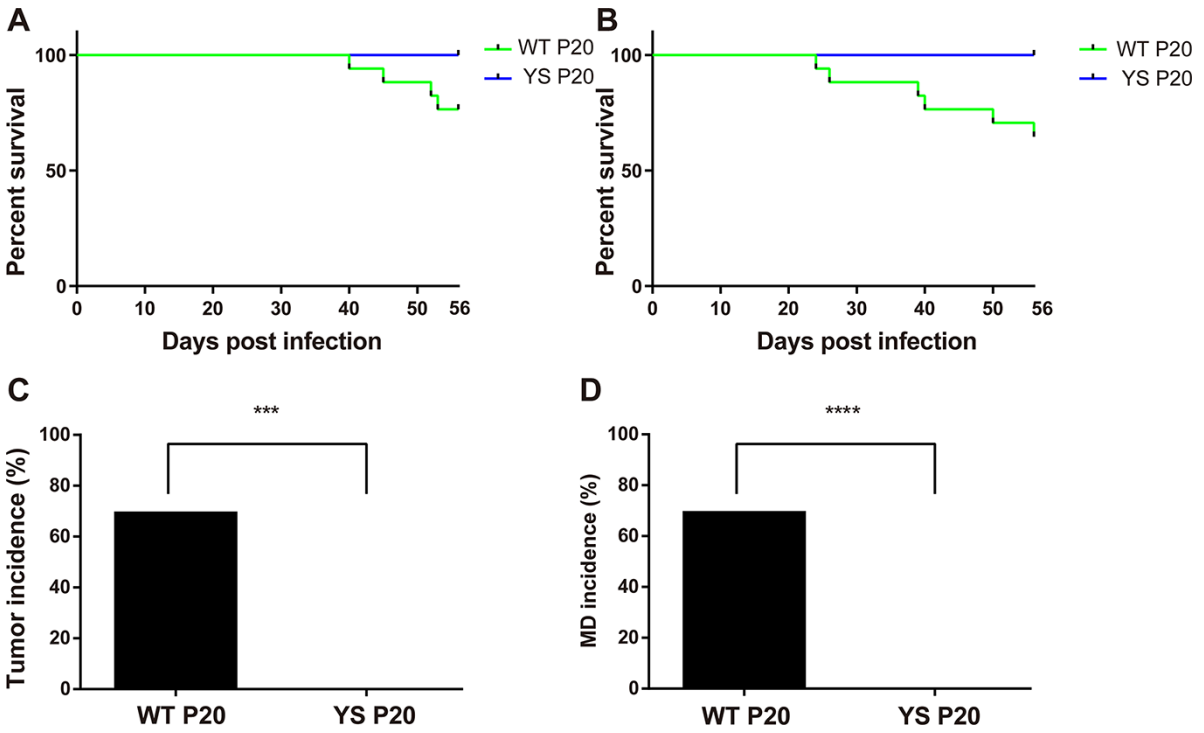

Figure 9. Survival analysis and tumor incidence of chickens infected with T7-adapted WT and Y547S viruses at P20. Survival curves for the first (A) and second (B) replicate of WT and Y547S infections are shown. Chickens were infected with indicated viruses at P20 of the first replicate of T7-adapted viruses. Animal numbers: WT P20 = 17; YS P20 = 17; Control = 10. Tumor incidences from the first (C) and second (D) replicate are shown as the percentage of affected chickens in each group. Asterisks indicate significant differences (*** $P < 0.001$, and *** $P < 0.0001$, Fisher's exact test).

we observe the influence of selective pressure on mutation frequency in this context, the ratio of mutations observed in Y547S vs. WT increased from 2.12 (CEC P60) to 4.95 (T7 P20). This indicates stronger selection for beneficial mutations and possibly also hitchhiking of neutral or even slightly deleterious mutations during adaptive processes required by novel host cells. Limited replication might also lead to bigger bottlenecks and therefore more genetic drift and accumulation of non-adaptive mutations (Manrubia et al. 2005; Lynch et al. 2016). These interpretations are further supported by the rapid accumulation of mutations in both WT and Y547S compared to CEC conditions. By P60 in CEC, the average accumulation rates of mutations in WT and Y547S are 0.48 and 1.01 mutations/passage, respectively; however, mutations accumulate in T7 cells by P20 at 0.95 and 4.70 mutations/passage for WT and Y547S, respectively (Supplementary Table S6). Not surprisingly, this adaptation to T7 cells comes with the cost of losing some replicative fitness on CECs. Of note, both the MDV WT and Y547S are able to adapt to growth in novel host cells with a striking pattern of penetrant mutations within MDV072. MDV072, encoding LORF11, is a unique gene of MDV and encodes a predicted protein of 903 amino acids. Little is known about the function of this gene; however, it was previously linked to cell tropism of the highly cell associated MDV (Lee et al. 2007) and might play an important role in adaptation to novel host cells.

We could further confirm that, in line with previous reports (Resch et al. 2020), *in vitro* passaging leads to attenuation *in vivo*. Our data show that attenuation is a function of passaging time, as virulence gradually decreased from P10 over P30 to P60 for both viruses. This effect was again more pronounced in Y547S, which suggests that even though the hypermutator is similarly fit *in vitro* compared to WT, the higher mutational load can cause stronger attenuation *in vivo*. Adaptation to non-permissive cells greatly accelerated this effect. The hypermutator Y547S became fully attenuated within only twenty passages, and infection with Y547S from P20 caused no apparent sign of disease in any of the infected animals in both replicates. In line with this view, mutational load in T7-adapted Y547S virus was even higher than in the P60 CEC virus, providing a genetic reason for the faster attenuation observed in this virus. Selection for mutations which enable infection of and replication in T7 are likely disadvantageous for *in vivo* replication in which intestinal epithelial cells play no important role. Therefore, the observed attenuation is probably a combination of the quantity as well as the specific effects of mutations accumulated *in vitro*.

In conclusion, the data presented here demonstrate how adaptation can be a function of mutation frequency. We could show better adaptation in the Y547S hypermutator if strong enough selection pressures were applied. Moreover, the evolutionary trade-off between replication on different cell types and between *in vitro* and *in vivo* growth is strongly reflected by our results. In the light of our findings on how hypermutation can accelerate evolutionary processes, hypermutator viruses could present and interesting tool for evolutionary virology. From studying antiviral resistance and the mechanism of attenuation in cell cultures, knowledge that could practically be exploited in rational drug and vaccine design, to immune evasion, spill-over events, and host jumps, many aspects of viral evolution could be studied more quickly and simply with hypermutator viruses. Unraveling the mechanisms of viral evolution, a field that still remains poorly understood, by means of hypermutation and selection under controlled laboratory conditions is a promising direction for future research.

Data availability

Raw sequencing data and alignments are available at the NCBI short read archive, BioProject PRJNA854607. Custom code used for data analysis is available at Github (https://github.com/mmnascimento/fastforwardingevolution).

Supplementary data

Supplementary data are available at *Virus Evolution* online.

Acknowledgements

We are grateful to Ann Reum, Annett Neubert, and Laurie Molitor for excellent technical assistance. We thank Dr. Michael Veit for providing T7 chicken intestinal epithelial cells. T.H., N.O., and D.P.M. were supported by the Volkswagenstiftung (Grant No. 96692).

Conflict of interest: None declared.

References

Bacon, L. D., Hunt, H. D., and Cheng, H. H. (2000) 'A Review of the Development of Chicken Lines to Resolve Genes Determining Resistance to Diseases', *Poultry Science*, 79: 1082–93.

Biggs, P. M. (2001) 'The History and Biology of Marek's Disease Virus', *Current Topics in Microbiology and Immunology*, 255: 1–24.

Blazquez, J. (2003) 'Hypermutation as a Factor Contributing to the Acquisition of Antimicrobial Resistance', *Clinical Infectious Diseases*, 37: 1201–9.

Blin, N., and Stafford, D. W. (1976) 'A General Method for Isolation of High Molecular Weight DNA from Eukaryotes', *Nucleic Acids Research*, 3: 2303–8.

Bolger, A. M., Lohse, M., and Usadel, B. (2014) 'Trimmomatic: A Flexible Trimmer for Illumina Sequence Data', *Bioinformatics*, 30: 2114–20.

Danecek, P. et al. (2021) 'Twelve Years of SAMtools and BCFtools', *Gigascience*, 1: giab008.

Gatherer, D. et al. (2021) 'ICTV Virus Taxonomy Profile: Herpesviridae 2021', *Journal of General Virology*, 102: 001673.

Graepel, K. W. et al. (2017) 'Proofreading-Deficient Coronaviruses Adapt for Increased Fitness over Long-Term Passage without Reversion of Exoribonuclease-Inactivating Mutations', *mBio*, 8: e01503–17.

Han, X., Bertzbach, L. D., and Veit, M. (2019) 'Mimicking the Passage of Avian Influenza Viruses through the Gastrointestinal Tract of Chickens', *Veterinary Microbiology*, 239: 108462.

Hildebrandt, E. et al. (2014) 'Characterizing the Molecular Basis of Attenuation of Marek's Disease Virus Via In Vitro Serial Passage Identifies De Novo Mutations in the Helicase-Primase Subunit Gene UL5 and other Candidates Associated with Reduced Virulence', *Journal of Virology*, 88: 6232–42.

Jarosinski, K. W. et al. (2005) 'Attenuation of Marek's Disease Virus by Deletion of Open Reading Frame RLORF4 but not RLORF5a', *Journal of Virology*, 79: 11647–59.

Lee, L. F. et al. (2007) 'Characterization of LORF11, A Unique Gene Common to the Three Marek's Disease Virus Serotypes', *Avian Diseases*, 51: 851–7.

Li, H., and Durbin, R. (2009) 'Fast and Accurate Short Read Alignment with Burrows-Wheeler Transform', *Bioinformatics*, 25: 1754–60.

Loewe, L., and Hill, W. G. (2010) 'The Population Genetics of Mutations: Good, Bad and Indifferent', *Philosophical Transactions of the Royal Society B: Biological Sciences*, 365: 1153–67.

Lynch, M. et al. (2016) 'Genetic Drift, Selection and the Evolution of the Mutation Rate', *Nature Reviews Genetics*, 17: 704–14.

Macia, M. D. et al. (2005) 'Hypermutation is a Key Factor in Development of Multiple-Antimicrobial Resistance in *Pseudomonas aeruginosa* Strains Causing Chronic Lung Infections', *Antimicrobial Agents and Chemotherapy*, 49: 3382–6.

Manrubia, S. C. et al. (2005) 'High Mutation Rates, Bottlenecks, and Robustness of RNA Viral Quasispecies', *Gene*, 347: 273–82.

Osterrieder, N. (1999) 'Sequence and Initial Characterization of the U(L)10 (Glycoprotein M) and U(L)11 Homologous Genes of Serotype 1 Marek's Disease Virus', *Archives of Virology*, 144: 1853–63.

——— et al. (2006) 'Marek's Disease Virus: From Miasma to Model', *Nature Reviews Microbiology*, 4: 283–94.

Osterrieder, N., and Vautherot, J. F. (2004) 'The Genome Content of Marek's Disease-Like Viruses'. In: D. Fred and N. Venugopal (eds) *Marek's Disease*, pp. 17–31. Elsevier.

Petherbridge, L. et al. (2004) 'Oncogenicity of Virulent Marek's Disease Virus Cloned as Bacterial Artificial Chromosomes', *Journal of Virology*, 78: 13376–80.

Reha-Krantz, L. J. (2010) 'DNA Polymerase Proofreading: Multiple Roles Maintain Genome Stability', *Biochimica et Biophysica Acta (BBA) – Proteins and Proteomics*, 1804: 1049–63.

Resch, T. K. et al. (2020) 'Serial Passaging of the Human Rotavirus CDC-9 Strain in Cell Culture Leads to Attenuation: Characterization from In Vitro and In Vivo Studies', *Journal of Virology*, 94: 15.

Robinson, J. T. et al. (2017) 'Variant Review with the Integrative Genomics Viewer', *Cancer Research*, 77: e31–4.

Sambrook, J., Russell, D. W., and Sambrook, J. (2006) *The Condensed Protocols: From Molecular Cloning: A Laboratory Manual*. New York: Cold Spring Harbor Laboratory Press Cold Spring Harbor.

Schumacher, D. et al. (2005) 'The Protein Encoded by the US3 Orthologue of Marek's Disease Virus is Required for Efficient De-Envelopment of Perinuclear Virions and Involved in Actin Stress Fiber Breakdown', *Journal of Virology*, 79: 3987–97.

Sheng, H. et al. (2020) 'Genes and Proteomes Associated with Increased Mutation Frequency and Multidrug Resistance of Naturally Occurring Mismatch Repair-Deficient Salmonella Hypermutators', *Frontiers in Microbiology*, 11: 770.

Sui, D. et al. (1995) 'Identification and Characterization of a Marek's Disease Virus Gene Encoding DNA Polymerase', *Virus Research*, 36: 269–78.

Trimpert, J. et al. (2017) 'A Phylogenomic Analysis of Marek's Disease Virus Reveals Independent Paths to Virulence in Eurasia and North America', *Evolutionary Applications*, 10: 1091–101.

——— et al. (2019) 'A Proofreading-impaired Herpesvirus Generates Populations with Quasispecies-like Structure', *Nature Microbiology*, 4: 2175–83.

Trimpert, J., and Osterrieder, N. (2019) 'Herpesvirus DNA Polymerase Mutants—How Important is Faithful Genome Replication?', *Current Clinical Microbiology Reports*, 6: 240–8.

Witter, R. L. (2001) 'Protective Efficacy of Marek's Disease Vaccines', *Current Topics in Microbiology and Immunology*, 255: 57–90.